ISSN 1990-7931, Russian Journal of Physical Chemistry B, 2008, Vol. 2, No. 1, pp. 115–122. © Pleiades Publishing, Ltd., 2008.
Original Russian Text © A.N. Novruzov, O.R. Rakhmanova, O.A. Novruzova, A.E. Galashev, 2008, published in Khimicheskaya Fizika, 2008, Vol. 27, No. 1, pp. 37–45.

CHEMISTRY
OF THE ATMOSPHERE

The Structure of Water Clusters Interacting with Gaseous Acetylene

A. N. Novruzov, O. R. Rakhmanova, O. A. Novruzova, and A. E. Galashev

Institute of Industrial Ecology, Ural Division, Russian Academy of Sciences, Yekaterinburg, 620219 Russia

Received October 4, 2006

Abstract—The interaction of water clusters with acetylene molecules at $T = 230$ K was studied by the molecular dynamics method. The structure of clusters was analyzed by constructing Voronoi polyhedra. Water clusters interacting with C_2H_2 molecules are characterized by a diversity of H-bond orientations, a more uniform distribution of H-bonds over the cluster volume, a larger number of bonds per atom, and smaller bond lengths. The spectrum of bond lengths broadens as the number of acetylene molecules interacting with the water cluster increases. C_2H_2 molecules have a pressing action on water clusters.

DOI: 10.1134/S199079310801017X

INTRODUCTION

Acetylene was observed in the atmosphere of giant planets such as Jupiter and Saturn and near large stars. It is supposed that, together with water, acetylene can form amino acids, which, in turn, transform into proteins and adenines, that is, basic DNA units. Spectroscopic measurements showed that water vapor was also present in the atmosphere of Jupiter. Acetylene was found in the atmosphere of the Earth and ice shells of comets. As distinct from the liquid and solid phases, the infrared (IR) spectra of gases are sets of vibrational-rotational bands whose shape depends on the moments of inertia of the molecule and its symmetry. For this reason, fundamentally new information related to the geometric structure of the complex can be extracted from the spectrum of the complex in the gas phase [1]. The IR spectra of acetylene contain two absorption bands. One band corresponds to stretching vibrations, and the other, to doubly degenerate bending vibrations. Carbon atoms are in the *sp* hybridization state in the acetylene molecule. This means that each carbon atom has two hybrid *sp* orbitals whose axes lie on the same line at an angle of 180° with respect to each other. Two *p* orbitals remain nonhybridized. Along one of the two hybrid orbitals of each C atom, overlapping occurs resulting in the formation of the *s* bond between carbon atoms. Each remaining hybrid orbital overlaps with the *s* orbital of the hydrogen atom to produce an *s* bond. Nuclear magnetic resonance spectra, which characterize the degree of nucleus screening by electrons, are evidence of a strong electron density shift from H to the C atom. The dipole moment of the acetylene molecule is 1.05 D [2]. The high polarity of the acetylene C–H bond is explained by a noticeable contribution of *s* orbitals to the hybrid orbital of carbon in acetylene (*sp* hybridization). Acetylene is poorly soluble in water, although better than methane and ethylene.

The shapes and positions of infrared absorption bands can be used to study the two-dimensional adsorption of acetylene in detail [3]. An effective method for studying ultrathin acetylene molecular layers is polarization infrared spectroscopy, especially in combination with low-energy electron diffraction or scattering of helium atoms [4]. The IR branch of the highest frequency (791 cm^{-1}) was found to be visible only in *p* polarization, because the induced dipole moment was perpendicular to the polarization plane [5]. The structure of deposited acetylene layers differs from the volume structure of orthorhombic acetylene. The short-range order of molecules having planar orientation in layers is determined by the T-shaped environment because of the predominance of quadrupole–quadrupole interactions. The angle made by adjacent molecule axes is 80°. A molecular dynamics study of the structure of acetylene films obtained on the (100) KCl plane is evidence that translational symmetry is sustained even in the 15th layer [5].

Because of their dipolar character, water molecules are especially capable of absorption. Water and gases, including C_2H_2, form gas hydrates under certain thermobaric conditions. These are crystalline compounds called clathrates. The interaction of disperse water medium with gaseous acetylene has been studied poorly.

The purpose of this work was to study the structural characteristics of water clusters colliding with acetylene molecules. Most attention was given to the character of changes in H-bonds in clusters, angular distribution of hydrogen atoms with respect to oxygen, the probability of formation of *m*-membered hydrogen rings, and the number of hydrogen atoms that bounded the region containing oxygen.

COMPUTER MODEL

The model was constructed on the basis of the well tested liquid water model [6] with an optimized set of TIP4P potential parameters. In addition to Lennard-Jones and Coulomb interactions, the model included polarization interactions. The first approximation to this model was the potential energy surface obtained in ab initio calculations [7]. The parameters were adjusted using high-level electronic structure calculations. The calculations were performed for a rigid four-center model of the water molecule. The geometry of the monomer in this model is constructed on the basis of the data obtained in studies of water in the gas phase. The O–H bond length was set at 0.09572 nm, and the H–O–H angle, at 104.5°. Fixed charges were assigned to hydrogen and the *M* point lying on the bisector of the H–O–H angle at a distance of 0.0215 nm from the oxygen atom. The charges ($q_H = 0.519e$, $q_M = -1.038e$) and position of point *M* were adjusted to reproduce both the experimental dipole and quadrupole moment values [8] and the energy and characteristic distances of the dimer obtained in ab initio calculations [9]. The characteristic distances for the C_2H_2 molecule are $r_{CC} = 0.121$ nm and $r_{CH} = 0.106$ nm [10]. The partial atomic charges play a very important role in analysis of the polarization properties of molecules. The charges at the centers of the C and H atoms are $q_H = 0.094e$ and $q_C = -0.094e$ [11]. The model presupposes calculations of the induced dipole moments of molecules, which allows the effect of their polarization to also be considered. This model well reproduces the structure and thermodynamic properties of massive water and water–vapor interface [6]. The optimized potential function also allows the structures of water clusters with minimum energies and bond energy to be reproduced correctly. The applicability of this model was substantiated in studies of the interaction of water clusters with nitrous oxide and methane molecules [12]. As in [11], the interaction of greenhouse gas molecules with water and each other is described in this work on the basis of the potentials calculated in the Gordon–Kim approximation with spherically averaged electron densities [11, 13]. The acetylene–water interaction was represented in the form of atom–atom interactions described by the sum of the repulsive, dispersion, and Coulomb contributions,

$$\Phi(r_{ij}) = b_i b_j \exp[-(c_i + c_j)r_{ij}] - a_i a_j r_{ij}^{-6} + \frac{q_i q_j}{r_{ij}},$$

where the a_i, b_i, and c_i parameters of the potential describing these interactions were taken from [13]. Although the polarizability of C_2H_2 molecules was 2.6 times higher than that of water, the induced dipole moment of water is on average two times higher than that of acetylene. This is caused by a close arrangement of H_2O molecules and some remoteness of C_2H_2 molecules from water.

First, we performed molecular dynamics calculations for water clusters. The final configuration of clusters was then used as the initial for the simulation of heteroclusters. In the initial state, the molecules to be added were arranged in such a way that the shortest distance between C_2H_2 atoms and the atoms of water molecules that formed a cluster be no less than 0.6 nm. The cutoff radius of intermolecular interactions was 0.9 nm. The linear C_2H_2 molecules attached were aligned with the rays that connected the center of mass of the water cluster with the centers of mass of these molecules.

The advantage of the model used over that employed in [6] was direct integration of the equations of motion for molecule rotations. The equations of motion of the centers of mass of molecules were integrated by the fourth-order Gear method [14]. An analytical solution to the equation of motion for rotations of molecules was obtained using the Rodrigues–Hamilton parameters [15], and the scheme for the integration of equations of motion including rotations corresponded to the approach suggested by Sonnenschein [16]. The temperature of clusters was the same in all calculations (230 K), and the duration of calculations for each cluster was no less than $2.5 \times 10^6\ \Delta t$, where the time step $\Delta t = 10^{-17}$ s. The calculations were performed on a Pentium-IV PC with a 3.8 GHz clock rate. The CPU time for calculations through $10^6 \Delta t$ for a cluster of 20 molecules was about 5 h.

One of the advantages of the polarization interaction potential that we used was the possibility of explaining the dipole moment value for each water molecule depending on the charges that surrounded it. In order to compare our model with one of the most popular nonpolarizable water models (SPC), we calculated the excess (with respect to the ideal gas) free energy ΔF of an extended system ($T = 273$ K) of 54 water molecules in a cubic cell [17]. The result ($\Delta F = -26.9$ kJ/mol) was in close agreement with the excess free energy ($\Delta F = -25.1$ kJ/mol) for the nonpolarizable model [18]. In the model that we used, the $\Delta F(t)$ function decreased more slowly at the initial stage of calculations and increased more slowly at the final stage.

The model of rigid molecules cannot be used to correctly calculate the IR spectrum of water at frequencies $\omega > 1200$ cm^{-1}, because the characteristic frequencies in this region are determined by intramolecular vibrations. Nor can the stretching vibrations of acetylene observed in its IR spectrum at 3287 cm^{-1} be considered in terms of this model [19]. Since the IR spectrum contains a large number of overtones and combination tones, we can suggest the following estimate of the frequency corresponding to one of the maxima in the IR spectrum of a water cluster with captured acetylene molecules. The intense band in the experimental IR absorption spectrum of water closest to the "threshold" frequency (1200 cm^{-1}) is observed at $\omega_1 = 1595$ cm^{-1}. A similar intense band of gaseous acetylene is situated at $\omega_2 = 729.1$ cm^{-1} [19]. Because of energy exchange with electromagnetic radiation, a photon with the frequency [20] $\omega = \omega_1 - \omega_2 = 865.9$ cm^{-1} is created. This

frequency is in satisfactory agreement with the position of the main maximum (930 cm^{-1}) in the IR absorption spectrum of the present model of disperse water medium with absorbed acetylene. The system of clusters whose molecules oscillate at an $\omega = 930$ cm^{-1} frequency is characterized by the period of oscillations ~0.036 ps. In this model, clusters do not decay over the time interval ~20 ps. During this period of time, molecules experience 550 characteristic vibrations. Let us consider the method for constructing a disperse system in more detail.

Three types of ultradisperse systems were studied. The first system contained water clusters of size from 10 to 20 molecules, the second one contained $C_2H_2(H_2O)_i$, $i = 10, \ldots, 20$ clusters, and the third system contained a set of $(C_2H_2)_2(H_2O)_i$ clusters also with i from 10 to 20. These systems will be denoted by I, II, and III, respectively. It was assumed that a cluster containing i admixture and n water molecules had the statistical weight

$$W_{in} = \frac{N_{in}}{N_{i\Sigma}}, \quad i = 0, 1, 2, \quad n = 10, \ldots, 20,$$

where N_{in} is the number of clusters with i admixture and n water molecules in 1 cm^3, $N_{i\Sigma} = \sum_{n=10}^{20} N_{in}$. The N_{in} value was estimated as follows. Let us consider nonpolarized light scattering, when the mean free path of molecules l is much smaller than the light wavelength λ. The extinction coefficient h of the incident ray is determined by the Rayleigh equation [21] on the one hand and through the scattering coefficient ρ $\left(h = \frac{16\pi}{3}\rho\right)$ [22] in the approximation of light scattering at a 90° angle on the other. Since $h = \alpha + \rho$, where α is the absorption coefficient, we have

$$N_{in} = \frac{2\omega^4}{3\pi c^4}\frac{(\sqrt{\varepsilon} - 1)^2}{\alpha}\left(1 - \frac{3}{16\pi}\right),$$

where c is the velocity of light, ε is the medium permittivity, and ω is the frequency of the incident wave. The spectral characteristics were calculated using the accepted statistical weights W_{in}. The formation of systems of clusters presupposes a uniform distribution of these formations. The corresponding model is valid at a low concentration of clusters at which they do not interact with each other. The mean concentration of clusters of each type in the systems studied was lower than the Loschmidt number by 12–13 orders of magnitude.

A STRUCTURAL ANALYSIS METHOD

A detailed study of the structure of clusters was performed by constructing Voronoi polyhedra. In crystals, the Wigner–Seitz cell is an analogue of the Voronoi polyhedron [23]. Voronoi polyhedra were constructed from the atomic coordinates recorded every 1000 time steps. The polyhedra were constructed around oxygen atoms closest to the center of mass of water clusters. The number of Voronoi polyhedra for each configuration was approximately equal to half the total number of oxygen atoms in the cluster. The special feature of these Voronoi polyhedra was the formation of their faces by hydrogen atoms surrounding the oxygen atom around which the Voronoi polyhedron was constructed. This approach was used because the number of hydrogen atoms in a water cluster was two times larger than the number of oxygens. In all probability, a completed Voronoi polyhedron can then be constructed. In addition, this polyhedron has a larger number of faces and a smaller volume and is more "spherical" than the Voronoi polyhedron constructed only using oxygen atom centers.

The degree of uniformity of the distribution of molecules with respect to the central molecule is characterized by Voronoi polyhedron "nonsphericity" determined by the equation [24]

$$\eta = \frac{S^3}{36V^2\pi},$$

where S is the polyhedron surface area and V is its volume. For instance, for a regular tetrahedron, η is 3.31.

However, oxygen was surrounded by the nearest hydrogen atoms largely because this allowed us to estimate the mean number $\bar{n}_b$ of H-bonds per atom if the nearest neighbors were selected properly. Proper selection is understood as the exclusion from neighbors of hydrogen atoms present together with oxygen in one H_2O molecule (the center of the Voronoi polyhedron). Fairly small faces were also excluded by eliminating edges of length $l < 0.5\bar{l}$, where $\bar{l}$ is the mean Voronoi polyhedron edge length. The use of this procedure often allows double bonds of a molecule with the oxygen atom under consideration to be removed. Voronoi polyhedra with excluded small edges will be called simplified. Nevertheless, the main point of the method for selecting nearest neighbors is the inclusion of only neighbors situated at a distance smaller than r_{min1} from the oxygen atom rather than all neighbors that form Voronoi polyhedron faces. Here, $r_{min1} = 0.25$ nm is the position of the first minimum of the partial radial distribution function $g_{OH}(r)$ of bulk water [25].

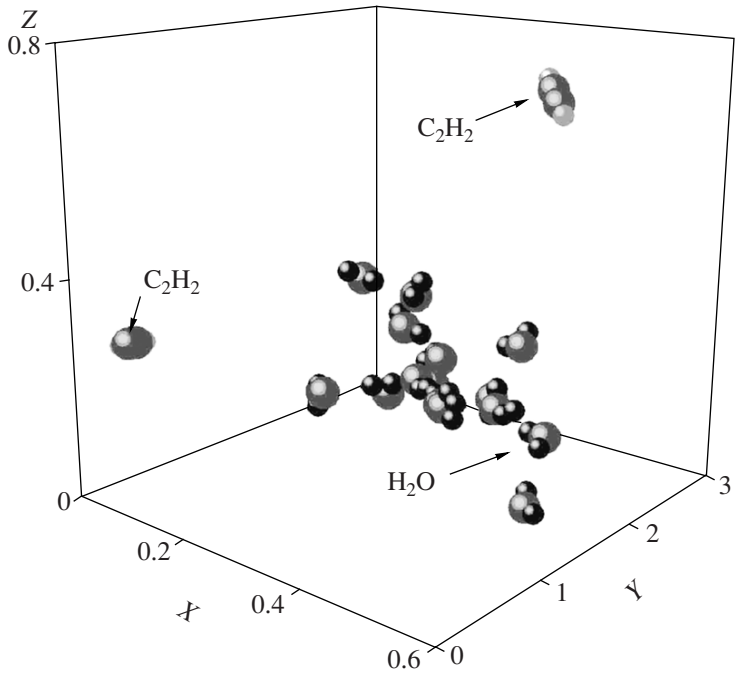

Fig. 1. Configuration of the $(C_2H_2)_2(H_2O)_{15}$ cluster at time 25 ps. The coordinates of molecules are given in $\sigma_w = 0.3234$ nm units (σ_w is the parameter of the Lennard-Jones part of the interaction potential for water).

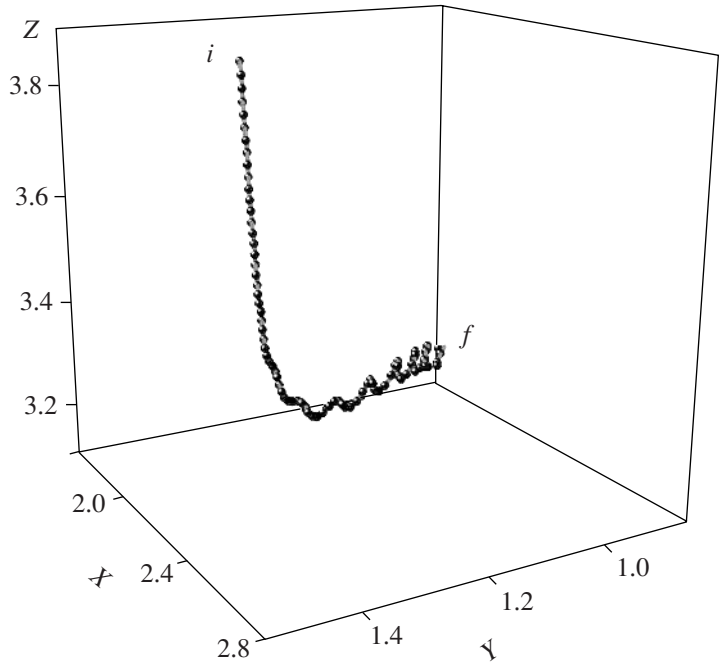

Fig. 2. Trajectory of the center of mass of C_2H_2 during 25 ps; *i* and *f* are the starting and end trajectory points, respectively; the coordinates are in σ_w units.

CALCULATION RESULTS

The orientation of C_2H_2 molecules with respect to the water cluster changed during simulations. For the larger period of time, acetylene molecules were directed parallel to the tangent to the surface of the cluster rather than toward its center of mass, like at the initial time. Such an orientation of C_2H_2 molecules can, in particular, be observed 25 ps after the beginning of calculations for the $(C_2H_2)_2(H_2O)_{15}$ cluster (Fig. 1).

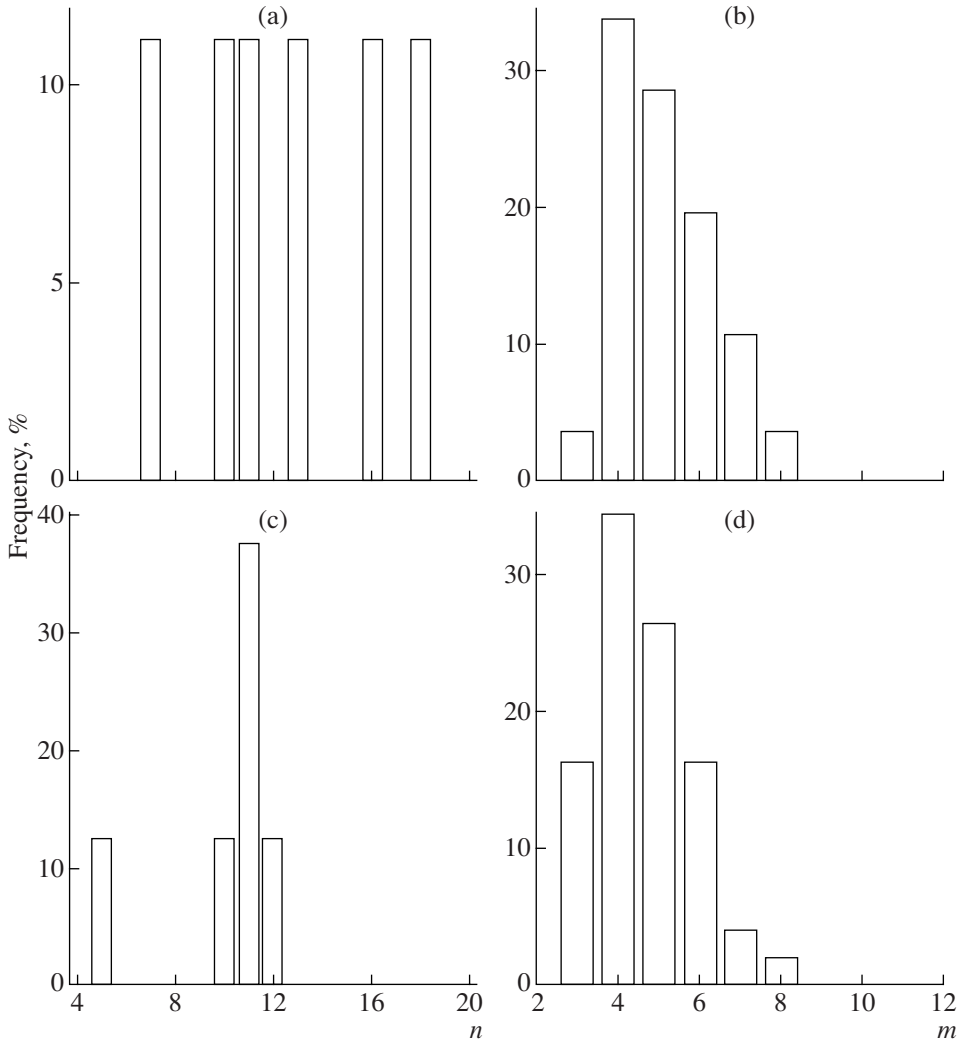

Fig. 3. Distribution of (a, c) simplified Voronoi polyhedra with respect to the number of faces and (b, d) faces with respect to the number of edges after the exclusion of edges of lengths $l \le 0.5\bar{l}$, where $\bar{l}$ is the mean polyhedron edge length for (a, b) $(H_2O)_{20}$ and (c, d) $C_2H_2(H_2O)_{20}$ clusters.

The motion of the center of mass of one of the C_2H_2 molecules in the formation of the $(C_2H_2)_2(H_2O)_{19}$ cluster is described by the trajectory shown in Fig. 2. The trajectory was tracked over 25 ps. The initial position of the center of mass of the molecule is denoted by *i*, and the final position, by *f*. We see that the C_2H_2 molecule first moves strictly rectilinearly toward the cluster. At a certain distance from it, the molecule turns in the direction of the tangent to the cluster surface and moves along this direction with small-scale oscillations.

The distribution of simplified Voronoi polyhedra with respect to the number of faces substantially changes already after the addition of one C_2H_2 molecule to a cluster (Figs. 3a, 3c). For the $(H_2O)_{20}$ cluster, simplified Voronoi polyhedra with 7, 10, 11, 13, 16, and 18 faces are equiprobable, whereas for the $C_2H_2(H_2O)_{20}$ cluster, simplified Voronoi polyhedra with 11 faces predominate. The composition of the faces of simplified Voronoi polyhedra does not change after the addition of a C_2H_2 molecule to the $(H_2O)_{20}$ cluster (Figs. 3b, 3d). The probabilities of the appearance of various faces in the Voronoi polyhedron of the $C_2H_2(H_2O)_{20}$ cluster are, however, somewhat different. In particular, the number of triangular faces increases from 3.5 to 16%, and the number of heptagons decreases from 10 to 4%. In both cases, quadrangular faces predominate in Voronoi polyhedra. The addition of two C_2H_2 molecules to the $(H_2O)_{20}$ cluster makes the *n* spectrum of simplified Voronoi polyhedra scanty (only penta- and dodecahedra remain), and its *m* spectrum is fully devoid of heptagons.

Figure 4 shows that the energy of Voronoi polyhedron faces changes substantially as the size of water clusters varies. The energy of true (not simplified) Voronoi polyhedron faces of water clusters is shown in

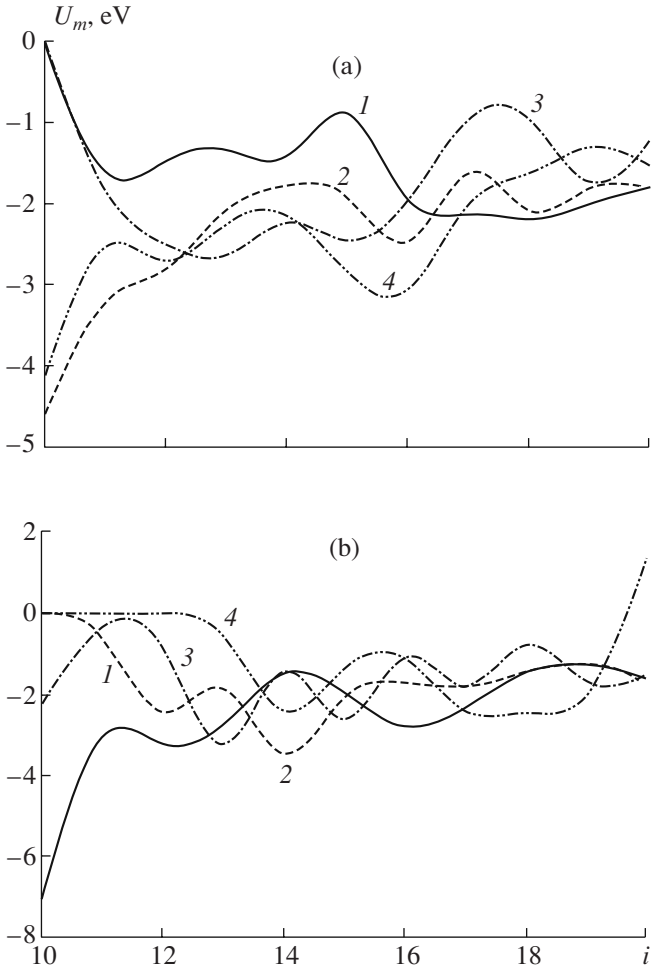

Fig. 4. Dependences of the energy of *m*-membered rings on the size (*i*) of water clusters; (a) *m* = (*1*) 3, (*2*) 4, (*3*) 5, and (*4*) 6; (b) *m* = (*1*) 7, (*2*) 8, (*3*) 9, and (*4*) 10.

the figure. A similar picture is observed for clusters containing C_2H_2 molecules. If a cluster contains no more than 12 H_2O molecules, quadrangular and heptagonal faces are most favorable energetically. For clusters with i = 19 and 20, triangular and nonagonal faces become energetically preferable. The lowest energy is that of heptagonal faces in polyhedra with 10 faces, and the highest energy is characteristic of decagonal faces in icosahedra.

The addition of C_2H_2 molecules to $(H_2O)_i$ clusters also substantially changes the angular distribution of the nearest hydrogen atoms around the center of the oxygen atom. In constructing angular distributions, we considered angles θ formed by pairs of hydrogen atoms selected in a Voronoi polyhedron and the vertex at the center of the oxygen atom. Figure 5 shows that already the presence of one C_2H_2 molecule in the $C_2H_2(H_2O)_{20}$ cluster considerably increases the number of peaks in the θ spectrum. The position of the main peak shifts from 96° to 102°. The probability of 180° angles becomes zero; that is, the nearest hydrogen atoms cannot be situated on a straight line passing through the oxygen atom center. The addition of two C_2H_2 molecules to $(H_2O)_i$ clusters makes the θ spectrum even more band-shaped.

The shape of Voronoi polyhedra is characterized by the nonsphericity η value. The behavior of this characteristic as the size of $(H_2O)_i$, $C_2H_2(H_2O)_i$, and $(C_2H_2)_2(H_2O)_i$ clusters changes because of the addition of water molecules is shown in Fig. 6. At sizes of $11 \le i \le 14$, the Voronoi polyhedra of pure water clusters is more nonspherical than the Voronoi polyhedra of clusters containing C_2H_2 molecules; that is, at such sizes, oxygens are surrounded by hydrogen atoms more uniformly when clusters contain acetylene molecules. However, at sizes of $15 \le i \le 18$, the Voronoi polyhedra

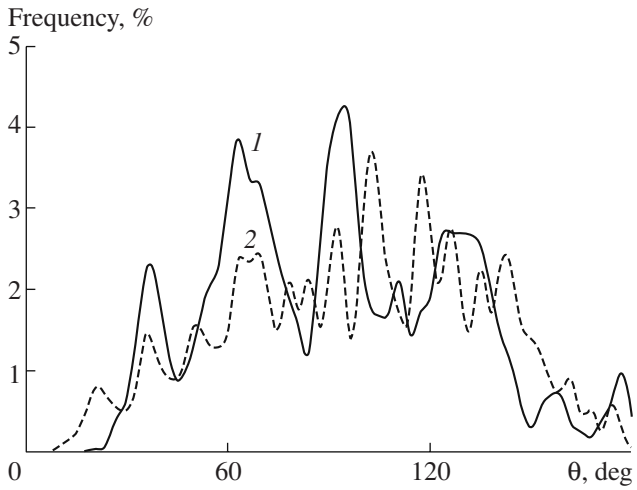

Fig. 5. Angular distribution of the nearest geometric neighbors in (*1*) $(H_2O)_{20}$ and (*2*) $C_2H_2(H_2O)_{20}$ clusters.

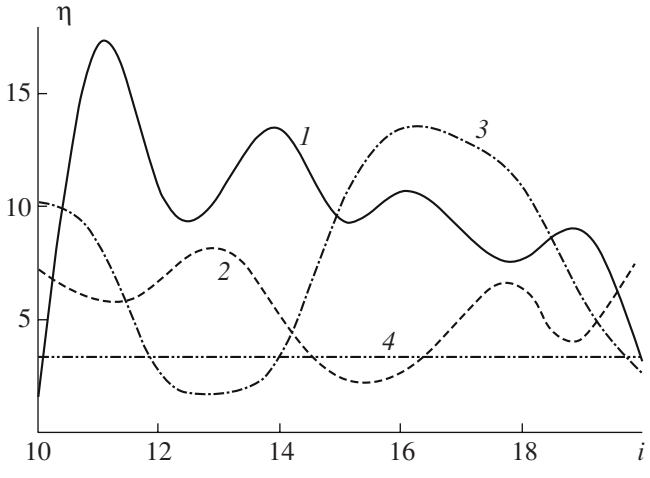

Fig. 6. Dependences of the nonsphericity coefficient of Voronoi polyhedra on the number i of water molecules in (*1*) $(H_2O)_i$, (*2*) $C_2H_2(H_2O)_i$, and (*3*) $(C_2H_2)_2(H_2)_i$ clusters and (*4*) the η coefficient for the regular tetrahedron.

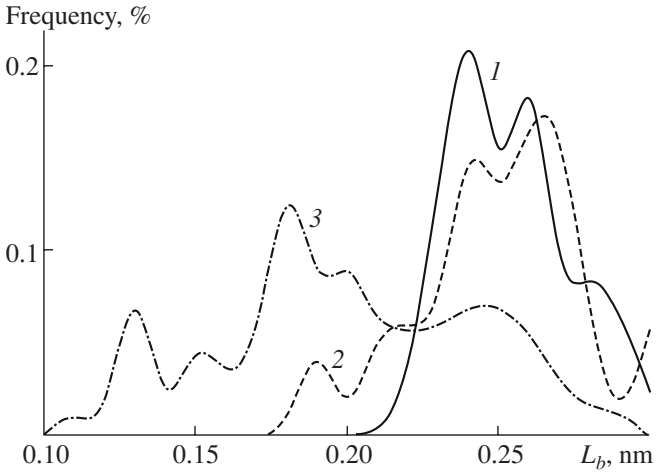

Fig. 7. H-bond length distributions in (*1*) $(H_2O)_{20}$, (*2*) $C_2H_2(H_2O)_{20}$, and (*3*) $(C_2H_2)_2(H_2O)_{20}$ clusters.

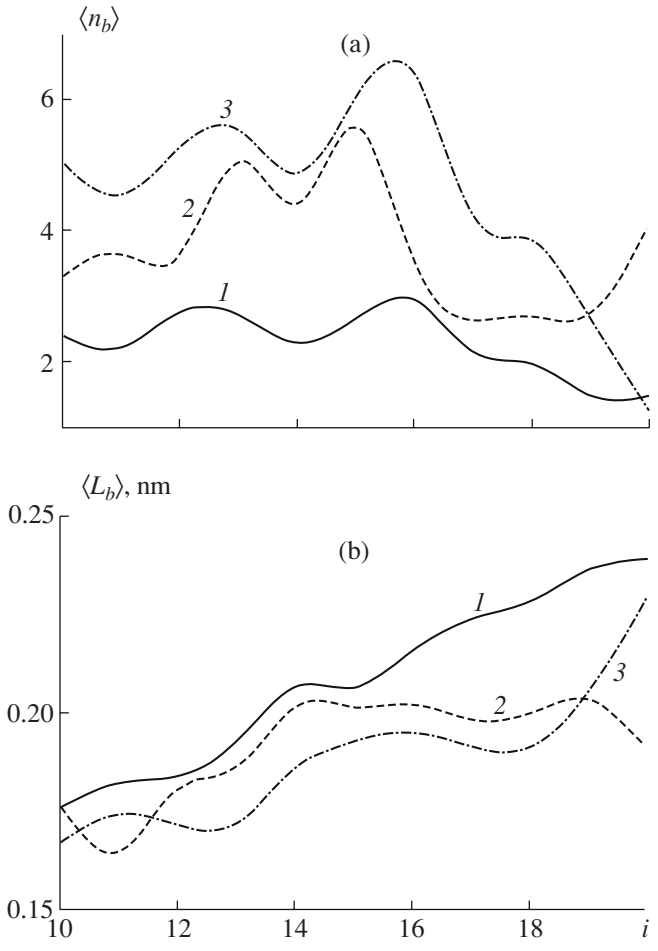

Fig. 8. Dependences of (a) the mean number of H-bonds per atom and (b) mean H-bond length on the number i of H_2O molecules in (*1*) $(H_2O)_i$, (*2*) $C_2H_2(H_2O)_i$, and (*3*) $(C_2H_2)_2(H_2O)_i$ clusters.

of clusters with two C_2H_2 molecules become more nonspherical, and, at $i = 20$, the Voronoi polyhedra of these clusters become the most spherical among the polyhedra of the types of clusters under consideration. The nonsphericity of the packing of water clusters containing less than 20 molecules, including clusters with C_2H_2 admixtures, is as a rule higher than the η coefficient for the regular tetrahedron. However, on the whole, the η coefficient exhibits a tendency to decrease as the size of clusters increases; that is, the $\eta(i)$ function tends to the η value for the regular tetrahedron as i increases. In other words, the growth of clusters contributes to an increase in the tetrahedral character of packing.

The distribution of H-bond lengths L_b in clusters containing 20 water molecules is shown in Fig. 7. The main distribution peak corresponds to 0.235 nm for pure water clusters and to 0.27 and 0.165 nm for clusters with one and two C_2H_2 molecules, respectively. The distribution of L_b for pure water clusters is characterized by the smallest variance, and that for clusters with two C_2H_2 molecules, by the largest variance. The extension of L_b distribution to smaller distances for clusters containing C_2H_2 molecules means that, on the whole, these molecules have a contracting action on ensembles of water molecules. This effect strengthens as the number of C_2H_2 molecules in water clusters increases.

The mean number of H-bonds per atom in the clusters and the mean length of H-bonds in them are shown in Fig. 8. The number of bonds $\bar{n}_b$ considerably increases after the addition of C_2H_2 molecules to water clusters. As a rule, the larger the number of C_2H_2 molecules added to a water cluster, the larger the $\bar{n}_b$ value for it. Clusters containing 15 and 16 water molecules have the largest $\bar{n}_b$ values, and clusters of size $i \geq 17$ are characterized by the smallest $\bar{n}_b$ values. The mean H-bond length on the whole increases as the size of the aggregate grows. This is not a monotonic dependence, and, for clusters containing one C_2H_2 molecule, L_b ceases to grow at i above 14. At all sizes, pure water clusters have the largest L_b values. The presence of C_2H_2 molecules shortens the mean length of H-bonds.

CONCLUSIONS

Acetylene molecules can fairly closely approach water molecules that form clusters and be held close to the surface of clusters for ~10 ps. C_2H_2 molecules do not penetrate into water clusters but experience translational and rotational motions close to their surface. These molecules are attracted to water clusters by their medium atoms, whereas their end atoms experience repulsion. In moving along a cluster, a C_2H_2 molecule is oriented parallel to the tangent to the cluster surface. The interaction of a water cluster with C_2H_2 molecules causes its thickening and makes the distribution of

hydrogen atoms nearest to oxygen more spherical. This is observed more often than the opposite effect. C_2H_2 molecules also noticeably change the orientation of H-bonds, increase their number, and shorten them. Lower temperatures would contribute to closer contacts of water clusters with C_2H_2 molecules. Such interactions are probable in the stratospheres of large planets.

The amount of heat supplied by the Sun per unit area of Jupiter is 51.0 W/m^2, which is 27 times lower than the amount of heat per unit area of the Earth. This heat is capable of heating the surface of Jupiter to an equilibrium temperature of 110 K. Measurements of infrared radiation from Jupiter are indicative of higher values, up to 170 K and even 270 K in certain regions. The equatorial regions of the stratosphere of Jupiter have a state close to equilibrium radiation. To describe the structure of the stratosphere of Jupiter more accurately, we must take into account the decay of C_2H_2 molecules in reactions with hydrogen. The photochemistry, radiation balance, and dynamics of the stratosphere of Jupiter are interrelated. When the number of water molecules in a cluster is not large ($i \le 20$), no solvation layer is formed around a C_2H_2 molecule brought in contact with the cluster; that is, no gas hydrate is formed. Under tropospheric conditions, the formation of gas hydrates, if possible, has a mechanism different from that governing the formation of clathrates. Gas hydrates are formed at higher pressures and can exist under nonequilibrium conditions at $T < 273$ K. They were, for instance, discovered in the frozen soil stratum. Under these conditions, the processes of the formation of pure ice and gas hydrates are similar in many respects.

ACKNOWLEDGMENTS

This work was financially supported by the Presidium of the Ural Division of the Russian Academy of Sciences (a grant for scientific projects of young scientists and postgraduates).

REFERENCES

1. *Spectroscopy of Interacting Molecules*, Ed. by M. O. Bulanin (Leningr. Gos. Univ., Leningrad, 1970) [in Russian].
2. L. A. Gribov, *Theory of Intensities in Infrared Spectra of Polyatomic Molecules* (Akad. Nauk SSSR, Moscow, 1963) [in Russian].
3. S. Hirabayashi, N. Yazawa, and Y. Hirahara, J. Phys. Chem. A **107**, 4829 (2003).
4. S. K. Dunn and G. E. Ewing, J. Phys. Chem. **96**, 5284 (1992).
5. J. Vogt, Phys. Rev. B: Condens. Matter **73**, 085418 (2006).
6. L. X. Dang and T.-M. Chang, J. Chem. Phys. **106**, 8149 (1997).
7. L. S. Sremaniak, L. Perera, and M. L. Berkowitz, J. Chem. Phys. **105**, 3715 (1996).
8. S. Xantheas, J. Chem. Phys. **104**, 8821 (1996).
9. D. Feller and D. A. Dixon, J. Chem. Phys. **100**, 2993 (1996).
10. *Handbook of Chemistry*, Ed. by B. P. Nikol'skii (Khimiya, Leningrad, 1971), Vol. 1 [in Russian].
11. M. A. Spackman, J. Chem. Phys. **85**, 6587 (1986).
12. A. E. Galashev, A. N. Novruzov, and O. A. Galasheva, Khim. Fiz. **25** (2), 26 (2006).
13. M. A. Spackman, J. Chem. Phys. **85**, 6579 (1986).
14. J. M. Haile, *Molecular Dynamics Simulation: Elementary Methods* (Wiley, New York, 1992).
15. V. N. Koshlyakov, *Problems of Rigid Body Dynamics and Applied Theory of Gyroscopes* (Nauka, Moscow, 1985) [in Russian].
16. R. Sonnenschein, J. Comp. Phys. **59**, 347 (1985).
17. A. E. Galashev, V. N. Chukanov, and O. R. Rakhmanova, in *Metastable States and Phase Transitions*, Ed. by E. N. Dubrovina (Nauchno-Izd. Sovet Ural. Otd. Ross. Akad. Nauk, Yekaterinburg, 2004), Vol. 7, p. 180 [in Russian].
18. J. Hermans, A. Pathiaseril, and A. Anderson, J. Am. Chem. Soc. **110**, 5982 (1988).
19. M. A. El'yashevich, *Atomic and Molecular Spectroscopy* (Gos. Izd. Fiz.-Mat. Lit., Moscow, 1962) [in Russian].
20. H. Poulet and J. P. Mathieu, *Vibrational Spectra and Symmetry of Crystals* (Gordon and Breach, Paris, 1970; Mir, Moscow, 1973).
21. L. D. Landau and E. M. Lifshitz, *Course of Theoretical Physics*, Vol. 8: *Electrodynamics of Continuous Media* (Nauka, Moscow, 1982; Pergamon, New York, 1984).
22. *Physical Encyclopedia*, Ed. by A. M. Prokhorov (Sovetskaya Entsiklopediya, 1988), Vol. 1 [in Russian].
23. J. M. Ziman, *Models of Disorder: the Theoretical Physics of Homogeneously Disordered Systems* (Cambridge University Press, Cambridge, 1979; Mir, Moscow, 1982).
24. N. N. Medvedev, *Voronoi–Delone Method in Investigation of the Structure of Noncrystalline Systems* (Sib. Otd. Ross. Akad. Nauk, Novosibirsk, 2000) [in Russian].
25. J. M. M. Cordeiro, Quim. Nova **21** (6), 1 (1998).